



**HAL**  
open science

## Inverse Gas Chromatography with Film Cell Unit: An Attractive Alternative Method to Characterize Surface Properties of Thin Films

Géraldine L. Klein, Pierre G, Marie-Noëlle Bellon-Fontaine, Marianne Graber

► **To cite this version:**

Géraldine L. Klein, Pierre G, Marie-Noëlle Bellon-Fontaine, Marianne Graber. Inverse Gas Chromatography with Film Cell Unit: An Attractive Alternative Method to Characterize Surface Properties of Thin Films. *Journal of Chromatographic Science*, 2015, 53 (8), pp.1233-1238. 10.1093/chrom-sci/bmv008 . hal-01247054

**HAL Id: hal-01247054**

**<https://hal.science/hal-01247054>**

Submitted on 21 Dec 2015

**HAL** is a multi-disciplinary open access archive for the deposit and dissemination of scientific research documents, whether they are published or not. The documents may come from teaching and research institutions in France or abroad, or from public or private research centers.

L'archive ouverte pluridisciplinaire **HAL**, est destinée au dépôt et à la diffusion de documents scientifiques de niveau recherche, publiés ou non, émanant des établissements d'enseignement et de recherche français ou étrangers, des laboratoires publics ou privés.

1 **Inverse Gas Chromatography with film cell unit: an attractive alternative method to**  
2 **characterize surface properties of thin films.**

3

4 Klein, G.L.<sup>1</sup>, Pierre, G.<sup>1</sup>, Bellon-Fontaine, M.N.<sup>2</sup>, Graber, M.<sup>1\*</sup>

5

6 (1) UMR 7266 CNRS - ULR LIENSs, Equipe Approches Moléculaires Environnement Santé. Université de La  
7 Rochelle, UFR Sciences, Bâtiment Marie Curie, avenue Michel Crépeau, 17042 La Rochelle, France.

8 (2) UMR 0763 – MICALIS - Agro-ParisTech-INRA – Equipe Bioadhésion-Biofilm et Hygiène des Matériaux, 25  
9 avenue de la république, 91300 Massy, France.

10 \*corresponding author, email : [mgraber@univ-lr.fr](mailto:mgraber@univ-lr.fr), tel: +33 5 46 45 86 30, fax: +33 5 46 45 82 65

11

12

**13 Abstract**

14 Inverse gas chromatography (IGC) is widely used for the characterization of surfaces. The present work describes a  
15 novel IGC tool, the recently developed film cell module, which measures monolithic thin solid film surface properties,  
16 whereas only samples in powder or fiber state or polymer-coated supports can be studied by classic IGC. The surface  
17 energy of four different solid supports was measured using both classic IGC with columns packed with samples in the  
18 powder state, and IGC with the new film cell module or the sessile drop technique, using samples in the film state. The  
19 total surface energy and its dispersive and specific components, were measured for Glass, Polyethylene, Polyamide and  
20 Polytetrafluoroethylene. Similar results were obtained for the four materials using the three different techniques. The  
21 main conclusion is that the new film cell module for IGC is an attractive alternative to the sessile drop technique as it  
22 gives very accurate and reproducible results for surface energy components, with significant savings in time and the  
23 possible control of sample humidity and temperature. This film cell module for IGC extends the application field of  
24 IGC to any thin solid film and can be used to study the effect of any surface treatment on surface energy.

25

26 *Keywords: Inverse gas chromatography, film sample, surface energy, contact angle.*

27

**28 Introduction**

29 Surface energy measurements are very frequently used in material sciences to investigate wettability, adhesion  
30 characteristics, specific interactions with other molecules, cohesion and coating performance [1]. The most commonly  
31 used method to achieve such measurements is the Sessile Drop Technique using a goniometer which is relatively easy to  
32 perform and inexpensive. It consists of producing a drop of liquid on a solid and measuring the angle formed between  
33 the solid/liquid interface and the liquid/vapor interface, which is called the “contact angle” (CA) [2]. This angle,  
34 measured for a minimum of three types of liquids, and the known surface energy of the liquids are the parameters that  
35 are used to calculate the surface energy of the solid sample [3]. The main disadvantage of this method is that it is unable  
36 to reflect the totality of the surface energy properties, even if multiple droplets are deposited on various locations on the  
37 sample. CA gives reproducible results, but problems of reproducibility and accuracy may occur, in case of droplets that  
38 are not axially symmetric, or with surface-accessible pores, which can decrease the droplet volume by capillary action  
39 during measurement [4,5]. To overcome these disadvantages, alternative methods of measuring surface energy must be  
40 developed. Two of the most common alternative methods are capillary intrusion of liquid analytes into the sample and  
41 analyte adsorption onto a sample bed at infinite dilution using Inverse Gas Chromatography (IGC). Capillary intrusion  
42 and conventional IGC are both restricted to the samples in the powder or fiber state and also to polymers and polymer-

43 coated supports, either packed in columns or deposited as a film on the inside of a column to create a capillary column.  
44 Nevertheless, a significant advance has been made recently with the development of a new system called film cell  
45 module for IGC, which is convenient for flat and monolithic samples. That is why we chose to focus on this last method  
46 as an alternative to CA measurements.

47 IGC is a vapor adsorption technique, which consists in an inversion of conventional gas chromatography. Physico-  
48 chemical characteristics in the stationary phase are studied by injecting specific well-characterized gaseous probes [6-  
49 8]. IGC is conventionally performed in columns containing the packed solid under investigation in the powder or fiber  
50 state. The interaction between these probes and the solid material forming the stationary phase is then investigated by  
51 determining the retention time for a given probe and used to calculate many physico-chemical properties, such as  
52 surface energies of solids [9], enthalpy and entropy adsorption [10], solubility parameter, crystallinity [11], surface  
53 heterogeneity [12], nanorugosity [11], glass transition [11] and melting temperature [7].

54 For surface energy determination, IGC presents many advantages compared to CA measurements: (i) the ability to  
55 quantify strong interaction occurring between the solid and the probes that cannot be characterized by contact angle  
56 measurement because of a contact angle close to zero [11], (ii) no problem of nanorugosity and surface heterogeneity  
57 [13,14], as the interactions of the probes are measured all along a wide solid surface and give mean values of interaction  
58 through the measure of the retention times, whereas CA measurements are restricted to the number of droplets  
59 deposited on the surface. Film cell module for IGC provides quite a large interacting area with gaseous probes: a  
60 relatively large rectangular sheet of flat sample (10 x 400 mm) is submitted to a gaseous flow carrying the probes,  
61 which are situated in a small groove all along the sample (iii) IGC is less time consuming, (iv) IGC is an accurate,  
62 versatile, reproducible method, with relatively easy sample preparation, (v) advanced IGC instruments have been  
63 developed with fully automated operation, humidity and temperature control, *in-situ* sample preconditioning; thus  
64 experiments may be carried out over appreciable temperature ranges, so that the temperature dependence of  
65 thermodynamic interactions can be determined.

66 The field of application of conventional IGC is wide. It concerns materials in the powder or fiber state and also  
67 polymers, that are either coated onto inert support and packed into columns or deposited as a uniform film on the inside  
68 of a column to create a capillary column [15]. It includes synthetic and biological polymers [8], paper and other  
69 cellulose, fillers and pigments, flavourings and perfumes, minerals and inorganic materials [16], food products [17],  
70 packaging and coatings, pharmaceuticals and medical products [18], building materials, cosmetics and ingredients,  
71 natural and artificial fibers [19], supported catalysts and microporous material [20] and adsorbents [21]. The new film  
72 cell module for IGC is able to extend these different application fields to monolithic thin solid films.

73 In the present work, we compare three approaches to determine the surface energy of solids, including the dispersive

74 and specific components: (i) conventional IGC at infinite dilution (IGC-C) with solid samples in the powder state  
75 packed in a column as a fixed bed, (ii) two-dimension IGC with the film cell module at infinite dilution (IGC-FC) with  
76 solid samples in the film state and (iii) analysis of CA data using the Good-van Oss theory, with solid samples in the  
77 film state. The surface energetics of four different materials including polymers (Polyamide (PA),  
78 Polytetrafluoroethylene (PTFE), and Polyethylene (PE) and glass were determined. These materials all exist in both  
79 powder and film states and their surface energy was investigated by the three IGC-C methods for powders and by IGC-  
80 FC and CA for films.

81 To our knowledge, no study has yet been devoted to the comparison of surface energy obtained for the same material in  
82 the granular state using IGC-C columns and in the film state using IGC-FC, nor to the comparison of surface energy  
83 values obtained by IGC-FC and CA for samples in the film state.

84

## 85 **Experimental**

86 All materials (powders or films) were washed as below. The sample was immersed in PCC-54 (Fisher Scientifics) 2 %  
87 (v/v) for 10 minutes with an orbital agitation (100 rpm, Heidolph Rotamax 120). Then they were rinsed five times with  
88 sterile ultrapure water at 40°C for 5 minutes with the same orbital agitation. Each film sample was finally wiped with  
89 optical cleaning tissue (Whatman 105), and was dried at 40°C into an incubator. All samples were stored at room  
90 temperature.

91 For CA measurements, a minimum of 10 droplets were measured on each surface.

92 All experiments involving IGC analysis were performed in triplicate, so a standard deviation can be calculated.

93

## 94 **Instrumentation and Reagents**

95 CA were measured with a goniometer G40 (Krüss, Germany) at room temperature (23°C) with an accuracy of  $\pm 2^\circ\text{C}$ .  
96 The chromatographic experiments were performed using an IGC 2000 (Surface Measurement Systems, London, UK). A  
97 technical drawing of the Film-cell module for IGC-FC (Surface Measurement Systems, London, UK) is presented in  
98 Figure 1. As an external bench-top unit made from stainless steel material, the film cell module provides an interacting  
99 area of 350 x 40 mm with a 0.3 mm groove.

100 The apolar probes (decane (C10), nonane (C9), octane (C8), heptane (C7) and hexane (C6)) and polar probes  
101 (dichloromethane, chloroform, ethyl acetate, toluene, diiodomethane and formamide) were supplied by Sigma with  
102 HPLC purity. They were used without further purifications. Ultrapure water was obtained via a Milli Q system  
103 (Millipore, France). The relevant characteristics of both amphoteric and polar probes, including the molecular cross-  
104 sectional surface area, the acid-base character and the surface energy components are presented in Table I.

105 Contact angle (CA), IGC-C and IGC-FC measurements were performed on four different supports: Glass (Thermo,  
 106 1mm thick), Polyethylene (PE, Goodfellow 0.5mm thick), Polyamide-nylon 6 (PA, Goodfellow 0.5 mm thick) and  
 107 Polytetrafluoroethylene (PTFE, Goodfellow 0.5 mm thick). For measurement by IGC-FC, the film materials was cut in  
 108 10 x 400 mm pieces, whereas IGC-C measurements in packed column were performed with the powders with particle  
 109 size ranging from 100 to 150  $\mu\text{m}$  of diameter. Packing is accomplished with the aid of a mechanical vibrator. For PE,  
 110 PA and PTFE, both powder and film had the same chemical composition. Both powder or film glass samples were made  
 111 in soda-lime-silica glass.

112

## 113 **Methods**

### 114 *Determination of surface energy by CA*

115 According to the GVOG (Good Van Oss Chaudhury) approach [3], CA were converted into surface energy components  
 116 using the Young-van Oss equation (Eq.1), which ignores spreading pressure and highlights Lifshitz-van der Waals and  
 117 Lewis acid/base surface free energy components.

$$118 \quad \gamma_L^t (1 + \cos \theta) = 2 \left( \sqrt{\gamma_s^{LW} \gamma_L^{LW}} + \sqrt{\gamma_s^+ \gamma_L^-} + \sqrt{\gamma_s^- \gamma_L^+} \right) \quad (1)$$

119 Here,  $\gamma^t$ ,  $\gamma^{LW}$ ,  $\gamma^+$  and  $\gamma^-$  are the total surface energy, Lifshitz-van der Waals, electron-acceptor (or Lewis-acid) and  
 120 electron-donor (or Lewis-base) components of the surface free energy respectively;  $\theta$  is the CA and the subscripts L and  
 121 S denote the liquid and solid samples, respectively.

122 Equation 2 allowed accessing to the Lewis acid-base components of the surface energy:

$$123 \quad \gamma^{AB} = 2\sqrt{\gamma^+ \gamma^-} \quad (2)$$

124

### 125 *Determination of surface energy by IGC*

126 IGC was operated at "infinite dilution.

#### 127 *Determination of the net retention volume*

128 The net retention volume  $V_N$  of vapor probes is then calculated using Eq.3 [22]:

$$129 \quad V_N = j \times t_N \times F \quad (\text{ml}) \quad (3)$$

130 where  $t_N$  is the net retention time, calculated using Eq. (4);  $F$  ( $\text{ml} \cdot \text{min}^{-1}$ ) the carrier gas flow rate, at the sample  
 131 temperature and  $j$  is the James and Martin compressibility factor, calculated using Eq. (5), taking into account the  
 132 compression of the gas and the pressure drop upstream the column or module [23].

133  $t_N = t_R - t_0$  (4)

134 where  $t_R$  is the experimental retention time used by a probe to cross the column or the film cell and  $t_0$  the dead time of  
135 the column or film cell, determined through the injection of methane which does not adsorb on the solid.

136 
$$j = \frac{3}{2} \times \frac{\left(\frac{P_i}{P_0}\right)^2 - 1}{\left(\frac{P_i}{P_0}\right)^3 - 1}$$
 (5)

137 where  $P_i$  and  $P_0$  are the inlet and outlet pressures respectively.

138 In practice,  $j$  is considered to be equal to 1 when using the film cell module.

139 *Determination of the free energy of adsorption*

140 The net retention volume  $V_N$  of vapor probes is directly related to the variation of the free energy of adsorption  $\Delta G_{ads}$ ,  
141 according to Eq.6

142 
$$\Delta G_{ads} = -(R \times T \times \ln V_N) + C$$
 (6)

143 where  $C$  is a constant depending on the choice of a reference state of the adsorbed probe and also on the total area of the  
144 solid accessible to the probe,  $R$  is the gas constant and  $T$  the absolute temperature.  $\Delta G_{ads}$  takes into account two kinds of  
145 interactions (Eq.7): dispersive interactions  $\Delta G_{ads}^D$ , corresponding to London forces and specific interactions  $\Delta G_{ads}^{SP}$ ,  
146 which consists mostly out in Lewis acid-base contributions.

147 
$$\Delta G_{ads} = \Delta G_{ads}^D + \Delta G_{ads}^{SP}$$
 (7)

148 To obtain the dispersive as well as the specific parts of  $\Delta G_{ads}$ , different apolar and polar vapor molecules respectively  
149 are injected and their net retention volume  $V_N$  determined.

150 *Determination of the dispersive component of the surface energy*

151 In case of apolar probes, like  $n$ -alkanes, which can only interact by dispersive interactions,  $V_N$  is related to  $\Delta G_{ads}^D$  by  
152 Eq.8, which uses the relation of Fowkes [24]:

153 
$$\Delta G_{ads}^D = -R \times T \times \ln V_N + C = -2N_A (\gamma_S^D)^{\frac{1}{2}} \times a \times (\gamma_L^D)^{\frac{1}{2}} + C'$$
 (8)

154 where  $N_A$  is the Avogadro constant,  $R$  the gas constant,  $a$  the molecular cross-sectional area of probes adsorbing on the  
155 solid surfaces ( $m^2$ ) and  $\gamma_L^D$  the dispersive component of the liquid probe surface energy and  $\gamma_S^D$  the dispersive

156 component of the surface energy of the solid. If a series of alkanes is injected,  $\gamma_S^D$  can be derived from the slope of the  
 157 fitted line, which is called the “alkane line” in a plot of  $RT \ln V_N$  versus  $a(\gamma_L^D)^{\frac{1}{2}}$ .

158 *Determination of the specific component of the surface energy*

159 The experimental points for the polar probe molecules are located above the alkane line in the surface energy plot. The  
 160 vertical distance between each point and the alkane straight line represents the specific contribution of the interaction,  
 161 which is expressed as the specific free energy  $\Delta G_{ads}^{SP}$ .

162 On the whole, this approach for acid-base calculations used in IGC is the van Oss concept, which provides acid and  
 163 base numbers in the same units as the dispersive surface energy, according to Eq.9:

$$164 \quad \Delta G_{ads}^{SP} = 2 \times N_a \times a \times \left( (\gamma_L^+ \times \gamma_S^-)^{\frac{1}{2}} + (\gamma_L^- \times \gamma_S^+)^{\frac{1}{2}} \right) \quad (9)$$

165 where  $\Delta G_{ads}^{SP}$  is the specific component of the surface energy (mJ/mol),  $N_A$  is the Avogadro constant,  $a$  the molecular  
 166 cross-sectional area of adsorbates (m<sup>2</sup>),  $\gamma_L^+$  and  $\gamma_L^-$  (mJ/m<sup>2</sup>) the electron acceptor (acid) and electron donor (base)  
 167 parameters of the probe molecule,  $\gamma_S^+$  and  $\gamma_S^-$  (mJ/m<sup>2</sup>) the electron acceptor (acid) and electron donor (base)  
 168 parameters of the surface. Then  $\gamma_S^+$  and  $\gamma_S^-$  can be calculated thanks to two couples of complementary polar probes:  
 169 dichloromethane (DCM)/ethyl acetate (EA) and toluene (T)/chloroform (CF), where  $\gamma_S^-$  is equal to zero for DCM and  
 170 CF and  $\gamma_S^+$  is equal to zero for EA and T.

171 The specific or polar component of surface energy  $\gamma_S^{SP}$  (mJ/m<sup>2</sup>) can then be calculated from the  $\gamma_S^+$  and  $\gamma_S^-$  according  
 172 to the Eq. 10. Finally, the total surface energy  $\gamma_S^t$  is also accessible through the Eq. 11.

$$173 \quad \gamma_S^{SP} = 2 \times \sqrt{\gamma_S^- \times \gamma_S^+} \quad (10)$$

$$174 \quad \gamma_S^t = \gamma_S^{SP} + \gamma_S^D \quad (11)$$

175

176 A conditioning period of 12 hours was applied for each experiment to equilibrate the chromatographic column or the  
 177 module with their sample *in situ* at constant conditions of temperature (40°C) and gas flow (helium, 10 mL/min) with a  
 178 relative humidity (RH) of zero, except when the effect of RH on surface energy was studied. In this case RH was equal



179 to values ranging from 10 to 50% in the carrier gas. The optimal quantity of probes to obtain an infinite dilution mode  
180 and sharp and symmetrical peaks were obtained at  $p/p_0 = 0.025$ , with  $p$  being the partial pressure of the solute in the gas  
181 phase and  $p_0$  the saturation vapor pressure of the solute.

182

183

## 184 **Results**

### 185 *Comparison of the surface energy obtained for materials in either the granular state using IGC-C columns or in the* 186 *film state using IGC-FC*

187 The main aim of this paper is to investigate the use of a new system called film cell module for IGC, to study the  
188 surface energetics of flat and monolithic samples. In order to assess whether meaningful data were obtained using this  
189 new module, the surface energetics of the same materials in either the granular state or in the film state were assessed by  
190 using respectively IGC-C and IGC-FC.

191 The IGC-FC method allows direct access to the surface energy of solid films. However, the use of the film cell module,  
192 which is made of stainless steel (Figure 1), leads to a measurement bias because it is not inert. The empty module has a  
193 significant polar component for its surface energy that must be subtracted by performing a blank. The dispersive  
194 component is, however, negligible. In contrast, IGC-C columns are made of inert glass and a blank is not necessary.

195 The results from both IGC-FC and IGC-C are summarized in Table II; the values of the total surface energy calculated  
196 from the IGC-FC experiments are in good agreement with those calculated from IGC-C for the different tested supports,  
197 except for PA. For this material, these values are equal to  $43.8 \pm 1.8$  mJ/m<sup>2</sup> from IGC-C and  $48.5 \pm 2.3$  mJ/m<sup>2</sup> from IGC-  
198 FC, respectively. The magnitude of all values determined here for all materials compared reasonably well with  
199 previously reported values in the literature [25].

200 For all the surface energy components measured in IGC-FC the calculated values are not significantly different from  
201 those obtained in IGC-C (Table II), except for PA and for the electron-donor component of glass. For PA, both  
202 dispersive and specific components of surface energy obtained from IGC-FC were higher than the ones obtained from  
203 IGC-C. For glass, the electron-donor component from IGC-C was higher than from IGC-FC.

### 204 *Comparison of the surface energy obtained by IGC-FC and CA for materials in the film state*

205 CA is one of the most commonly used techniques in the characterization of surface energetics and wettability of  
206 materials in the film state. It was therefore used as a point of comparison with IGC-FC. As observed in Table II, the  
207 values of the total surface energy calculated from the CA experiments corroborate the surface energy trends established  
208 with IGC-FC and give somewhat lower absolute values for these numbers, in case of the three substrata with the lowest

209 surface energy: PTFE, PE and PA. A GVOC approach was used for CA experiments, which allows the conversion of CA  
 210 into  $\gamma_S^{LW}$  (Lifshitz-van der Waals), and  $\gamma_S^+$  and  $\gamma_S^-$  (Lewis acid and base) surface energy components. It is recognized  
 211 that the Lifshitz-van der Waals contribution is primarily due to dispersion forces or London interactions, although small  
 212 contributions resulting from the presence of permanent dipoles may also be accounted for in this term (induction or  
 213 Debye and orientation or Keesom interactions) [26]. Therefore, it is relevant to compare values obtained from CA and  
 214 values obtained from IGC-FC.

215 For PTFE, PE and PA, the  $\gamma_S^D$  obtained using IGC-FC were slightly superior to the  $\gamma_S^{LW}$  values obtained from CA:  
 216 Interestingly, in the case of glass, a higher value for the total surface energy ( $\gamma_S^t = 56.2 \pm 0.3 \text{ mJ/m}^2$ ) was calculated  
 217 with CA measurements, compared to IGC-FC, for which a value of  $47.9 \pm 3.3 \text{ mJ/m}^2$  was obtained (Table II). This  
 218 difference is statistically significant with a *p-value* of 0.00021 (calculated from Student test). It arose only from the  $\gamma_S^-$   
 219 values that are equal to  $11.0 \pm 2.6 \text{ mJ/m}^2$  with IGC-FC and  $54.1 \pm 2.6 \text{ mJ/m}^2$  with CA, whereas  $\gamma_S^D$  and  $\gamma_S^{LW}$  values on  
 220 the one side and  $\gamma_S^+$  values on the other side were very similar.

221

### 222 *Effect of relative humidity on the surface energy of glass measured by IGC-FC*

223 The influence of the relative humidity (RH) on the evolution of the specific component of the surface energy for glass  
 224 was examined using IGC-FC.

225 The results for the total surface energy and its different components measured by IGC-FC as a function of RH are  
 226 presented in Figure 2. On the right of Figure 2 are also presented the results for the total surface energy and its different  
 227 components for glass measured by CA with atmospheric RH equal to 50%. For glass from IGC-FC measurements, it  
 228 appears that the electron-donor component significantly increases with the RH. On the other hand, the dispersive and  
 229 electron-acceptor components maintain similar values all along the humidity gradient. The values calculated for the  
 230 electron-donor component increased from  $11.0 \text{ mJ/m}^2$  to  $66.79 \text{ mJ/m}^2$  in accord with the gradient of RH in the gaseous  
 231 stream and from 0 to 50 %RH in IGC-FC, and showed a linear tendency between 10 and 50 %RH, with a slope equal to  
 232  $15.3 \text{ (mJ/m}^2\text{)/(\%RH)}$ . The increase in the electron-donor component with RH may be due to the interaction of the  
 233 probes with water molecules adsorbed on the surface and the formation of silanol (Si-O-H) sites by chemisorption. For  
 234 glass from CA measurements taken at room temperature with atmospheric RH equal to 50%, it appears that the value of  
 235 the electron-donor component is close to the one obtained with IGC-FC at 30 and 40%RH.

236

237

238 **Discussion**

239 As mentioned in the results part, the values obtained for surface energetics by IGC-FC corroborate those surface energy  
240 trends established with IGC-C and the magnitude of these numbers compare reasonably well. Some significant  
241 differences between the two methods exist however for the absolute values of both dispersive and specific components  
242 of surface energy found for PA and also for the electron-donor component of glass. These differences may arise from an  
243 effect of the geometry of the materials on the interpreted surface energetics, as shown previously for different works  
244 using IGC. For example, Guillet et al. reported differences for polystyrene between studies using pure polymer packed  
245 in a column and or capillary columns coated on the inside with polymer [15]. They found that specific retention volume  
246 values were slightly higher for an open column than for a packed column, possibly because of the higher specific  
247 surface area available in the open column. Jones et al. mention that milling increased the dispersive surface energy and  
248 surface acidity of lactose and several respiratory drugs. These effects could be ascribed to the introduction of surface  
249 structural defects or to the disruption of particle flaws exposing surfaces rich in hydroxyl groups in the case of lactose  
250 [18].

251 The differences between results from CA and IGC are well known and the discussion about this point is out of the scope  
252 of this paper. These differences arise from the vastly different energetics between the two systems, involving  
253 gas/condensed phase interaction for IGC and condensed phase/condensed phase interaction for CA. In the present study,  
254 another difference was introduced between the two systems through the difference in RH values during experiments:

255 RH was not controlled during CA experiments and was equal to the ambient atmospheric RH which was 50% that day.

256 This is one of the reasons explaining the important difference in the  $\gamma_s^-$  values found for glass using CA or IGC at RH  
257 equal to 0. Glass is by far the most hydrophilic material among the four studied. It is composed mainly of silica, and  
258 previous studies have shown that water can rupture siloxane (Si-O-Si) bonds via dissociative chemisorption, forming  
259 silanol (Si-O-H) sites, in particular at the first stage of humidification [27,28]. This chemical change occurring at the  
260 surface of glass also affects the specific component of the surface energy. For this reason, the effect of RH on the  
261 surface energy was studied for glass by IGC-FC. It appears that when increasing the RH from 0 to 50% in IGC, the  
262 difference in the  $\gamma_s^-$  values found for glass using CA or IGC-FC decreases. However, considering that temperature is  
263 changed from 23°C to 40°C between CA and IGC-FC experiments, the quantity of adsorbed water on glass for a same  
264 RH is higher in case of IGC-FC, undercutting the relevance of the exact comparison of results from CA and IGC-FC at  
265 the same RH.

266

267 **Conclusion**

268 The new film cell module for inverse Gas Chromatography experiments, presented in this work, enables to obtain  
269 meaningful data for the surface energetics of flat and monolithic samples, for solid materials with varying surface  
270 properties: PTFE, PE, PA and glass. In comparison with CA measurements, it offers the possibility to control the  
271 temperature and the RH perfectly during automated and rapid experiments, including *in situ* conditioning.

272 Thanks to these preliminary results, it can be concluded that IGC-FC appears as a viable method. However, more  
273 extensive study is needed to identify the origin of differences with standard IGC-C, since the differences in surface  
274 geometry may also have an influence on the interpreted surface energetics. IGC-FC extends the possibility of IGC to  
275 flat and monolithic samples. The analysis can be performed directly on two dimensions samples, without any prior  
276 preparation. The field of application of IGC-FC is large and includes the easy analysis of the influence of cleaning or  
277 painting on the surface energy parameters of solid surfaces, important in a wide variety of industries.

278

279 **Acknowledgment**

280 Financial support for this work was received from the Conseil Général de Charente-Maritime through the Contrat de  
281 Projet Etat-Région (CPER) Littoral. Dr Majid Naderi and Pramod Kerai (Surface Measurement Systems Ltd., London,  
282 U.K.) are thanked for helpful advice about film cell use. The manuscript was corrected by a native English speaking  
283 scientific translator (<http://traduction.lefevere-laoide.net>).

284

285 **References**

286 [1] Good, R.J.; Contact-angle, wetting and adhesion – A critical review; *Journal of Adhesion Science Technology*,  
287 (1992); 6:1269-1302.

288 [2] Zisman, W.A.; Fowkes, F.M. (ed.) Contact Angle, Wettability and Adhesion, Advances in Chemistry Series, Vol. 43,  
289 American Chemical Society, Washington D.C., (1964).

290 [3] van Oss, C.J., Chaudhury, M.K., Good, R.J.; Interfacial Lifshitz-van der Waals and polar interactions in macroscopic  
291 systems; *Chemical Reviews*, (1988); 88:927-941.

292 [4] Chini, S.F., Amirfazhi, A. ; A method for measuring contact angle of asymmetric and symmetric drops ; *Colloids and*  
293 *Surfaces A: Physicochemical and Engineering Aspects*, (2011); 388: 29-37.

294 [5] Wenzel, R.N.; Surface roughness and contact angle; *Journal of Physical and Colloid Chemistry*, (1949); 53:1466-  
295 1467.

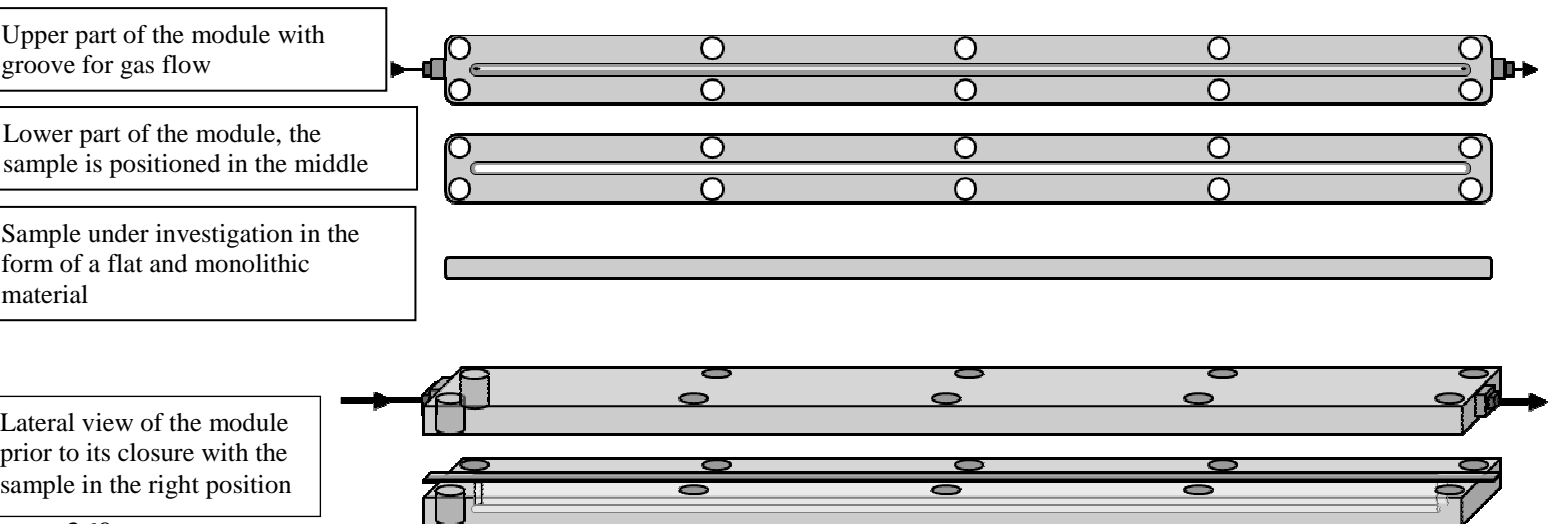
296 [6] Conder, J.R., Young, C.L.; Wiley, J. & Sons (ed). Physical measurements by gas chromatography, Wiley-

- 297 interscience, New-York, (1969).
- 298 [7] Hegedus, C.R., Kamel, I.L.; A review of inverse gas chromatography theory used in the thermodynamic analysis of  
299 pigment and polymer surfaces; *Journal of Coatings Technology*, (1993); 65:23-30.
- 300 [8] Voelkel, A.; Inverse gas chromatography: characterization of polymers, fibers, modified silicas, and surfacants;  
301 *Critical Reviews in Analytical Chemistry*, (1991); 22: 411-439.
- 302 [9] Huang, X., Shi, B., Li, B., Li, L., Zhang, X., Zhao, S.; Surface characterization of nylon 66 by inverse gas  
303 chromatography and contact angle; *Polymer Testing*, (2006); 25:970-974.
- 304 [10] Santos, J.M.R.C.A., Fagelman, K., Guthrie, J.T.; Characterisation of the surface Lewis acid-base properties of  
305 poly(butylene terephthalate) by inverse gas chromatography; *Journal of Chromatography A*, (2002); 969:111-118.
- 306 [11] Santos, J.M.R.C.A., Guthrie, J.T.; Analysis of Interactions in Multicomponent Polymeric Systems: The Key-role of  
307 Inverse Gas Chromatography; *Materials Science and Engineering Reports*, (2005); 50:79-81.
- 308 [12] Gavril, D., Nieuwenhuys, B.E.; Investigation of the surface heterogeneity of solids from reversed-flow inverse gas  
309 chromatography; *Journal of Chromatography A*, (2004); 1045:161-172.
- 310 [13] Brendlé, E., Papirer, E.; A new topological index for molecular probes used in inverse gas chromatography for the  
311 surface nanorugosity evaluation, 1. Method of evaluation; *Journal of Colloid and Interface Science*, (1997a); 194:207-  
312 216.
- 313 [14] Brendlé, E., Papirer, E.; A new topological index for molecular probes used in inverse gas chromatography, 2.  
314 Application for the evaluation of the solid surface specific interaction potential; *Journal of Colloid and Interface  
315 Science*, (1997b); 194:217-224.
- 316 [15] Guillet, J.E., Romansky, M., Price, G.J., van der Mark, R.; Studies of Polymer Structure and Interactions by  
317 Automated Inverse Gas Chromatography. In *Inverse Gas Chromatography, Characterization of Polymers and Other  
318 Materials*, Chapter 3. ACS symposium Series 391, American Chemical Society: Washington, DC, (1989), pp. 20-32.
- 319 [16] Papirer, E., Brendlé, E., Ozil, F., Balard, H.; Comparison of the surface properties of graphite, carbon black and  
320 fullerene samples, measured by inverse gas chromatography; *CARBON*, (1999); 7:1265-1274.
- 321 [17] Boutboul, A., Giampaoli, P., Feigenbaum, A., Ducruet, V.; Influence of the nature and treatment of starch on aroma  
322 retention; *Carbohydrate Research*, (2002); 47:73-82.
- 323 [18] Jones, M.D., Young, P., Traini, D.; The use of inverse gas chromatography for the study of lactose and  
324 pharmaceutical materials used in dry powder inhalers; *Advanced Drug Delivery Reviews*, (2012); 64:285-293.
- 325 [19] Vega, A., Diez, F.V., Hurtado, P., Coca, J.; Characterization of polyarylamide fibers by inverse gas  
326 chromatography; *Journal of Chromatography A*, (2002); 962:153-160.
- 327 [20] Marton, Z., Chaput, L., Pierre, G., Graber, M.; Lipase hydration in the gas phase: Sorption isotherm measurements

- 328 and inverse gas chromatography; *Biotechnology Journal*, (2010); 5:1216-1225.
- 329 [21] Elizalde-Gonzalez, M.P., Ruiz-Palma, R.; Gas chromatographic characterization of the adsorption properties of the  
330 natural adsorbent CACMM2; *Journal of Chromatography A*, (1999); 845:373-379.
- 331 [22] Schultz, J., Lavielle, L., Martin, C.; Surface properties of carbon-fibers determined by inverse gas  
332 chromatography; *Journal of Chemical Physics*, (1987); 84:231-237.
- 333 [23] James, A.T., Martin, J.P.; Gas-liquid partition chromatography: the separation and micro-estimation of volatile fatty  
334 acids from formic acid to dodecanoic acid; *Biochemical Journal*, (1952); 50:679-690.
- 335 [24] Fowkes, F.M.; Additivity of intermolecular forces at interfaces. 1. Determination of contribution to surface and  
336 interfacial tensions of dispersion forces in various liquids; *Journal of Physical Chemistry*, (1963); 67:2538-2541.
- 337 [25] Kinloch, A.J.; Adhesion and Adhesives: Science and Technology, Chapman and Hall, London, (1987).
- 338 [26] Steele, D.F., Moreton, R.C., Staniforth, J.N., Young, P.M., Tobyn, M.J., Edge, S.; Surface Energy of  
339 Microcrystalline Cellulose Determined by Capillary Intrusion and Inverse Gas Chromatography; *The AAPS Journal*,  
340 (2008); 10:494-503.
- 341 [27] Sun, C., Berg, J.C.; Effect of moisture on the surface free energy and acid-base properties of mineral oxides;  
342 *Journal of Chromatography A*, (2002); 969:59-72.
- 343 [28] Mahadevan, T.S., Garofalini, S.H.; Dissociative Chemisorption of Water onto Silica Surfaces and Formation of  
344 Hydronium Ions; *The Journal of Physical Chemistry C*, (2008); 112:1507-1515.
- 345 [29] Hefer, A.W., Little, D.N., Herbert, B.E.; Bitumen surface energy characterization by inverse gas chromatography;  
346 *Journal of Testing and Evaluation*, (2007); 35:233-239.
- 347 [30] Della Volpe, C., Siboni, S.; Some reflections on acid-base solid surface free energy theories; *Journal of Colloid and*  
348 *Interface Science*, (1997); 195:121-136.
- 349 [31] Schultz, J., Tsutsumi, K., Donnet, J.B.; Surface properties of high-energy solids I. Determination of the dispersive  
350 component of the surface free energy of mica and its energy of adhesion to water and n-alkanes; *Journal of Colloid and*  
351 *Interface Science*, (1977); 59:272-276.
- 352 [32] van Oss, C.J., Chaudhury, M.K., Good, R.J.; Monopolar surfaces; *Advances in Colloid and Interface Science*,  
353 (1987); 28:35-64.
- 354 [33] van Oss, C.J., Giese, R.F., Li, Z., Murphy, K., Norris, J., Chaudhury, M.K., Good, R.J.; Determination of contact  
355 angles and pore sizes of porous media by column and thin layer wicking; *Journal of Adhesion Science Technology*,  
356 (1992); 6:413-428.
- 357

358 Figure 1: Technical drawing of the film cell module for iGC (35x400x11 mm). The arrows show gas flow.

359

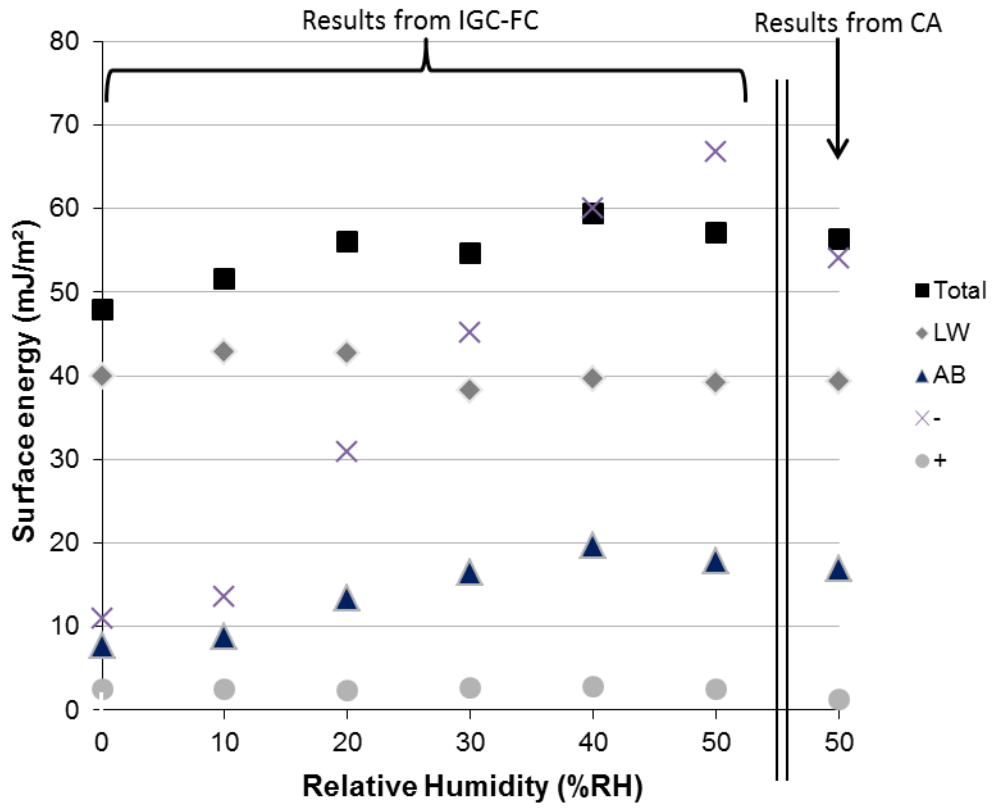


360  
361

362

363 Figure 2: Surface energy components measured on Glass, depending on a RH gradient established into the film cell  
 364 module during iGC experiments and values obtained with CA measurements at “ambient” RH.

365



366

367



368 Table I: Acid-base character and values of cross sectional area and surface energy components of amphoteric and polar  
 369 probes used in contact angle and IGC experiments. Values from [29-33], DCM = dichloromethane, EA = ethyl acetate,  
 370 T = toluene, CF = chloroform.

Solvents - probes	Molecular cross-sectional surface area "a" (m <sup>2</sup> )	Surface energy (mJ/m <sup>2</sup> ) of the liquid probes			
		total surface energy $\gamma_L^t$	dispersive component $\gamma_L^D$	electron acceptor parameter $\gamma_L^+$	electron donor parameter $\gamma_L^-$
<b><i>n</i>-alkanes</b>					
<b>C6</b>	5.15 x10 <sup>-19</sup>	18.4	18.4	0.0	0.0
<b>C7</b>	5.73 x10 <sup>-19</sup>	20.3	20.3	0.0	0.0
<b>C8</b>	6.30 x10 <sup>-19</sup>	21.3	21.3	0.0	0.0
<b>C9</b>	6.92 x10 <sup>-19</sup>	22.7	22.7	0.0	0.0
<b>C10</b>	7.44 x10 <sup>-19</sup>	23.9	23.9	0.0	0.0
<b>Contact angle</b>					
<b>water</b>	/	72.8	21.8	25.5	25.5
<b>formamide</b>	/	58.0	35.6	2.3	39.6
<b>diiodomethane</b>	/	50.8	50.8	0.0	0.0
<b>iGC</b>					
<b>DCM</b>	2.99 x10 <sup>-19</sup>	26.5	26.5	5.2	0.0
<b>EA</b>	3.29 x10 <sup>-19</sup>	23.9	23.9	0.0	19.2
<b>T</b>	4.20 x10 <sup>-19</sup>	28.5	28.5	0.0	2.3
<b>CF</b>	3.51 x10 <sup>-19</sup>	27.2	27.2	3.8	0.0

371

372 Table II: Calculated values of surface energy for five materials, PA = polyamide-6, PE = polyethylene, PTFE =  
 373 polytetrafluoroethylene and Glass. <sup>a</sup> Materials at powder state. <sup>b</sup> Materials at film state. Standard deviations were  
 374 calculated with  $n \geq 10$  measurements.

375

Materials	$\gamma_s^t$ (mJ/m <sup>2</sup> )	$\gamma_s^{LW}$ (mJ/m <sup>2</sup> ) (CA) $\gamma_s^D$ (mJ/m <sup>2</sup> ) (iGC)	$\gamma_s^{SP}$ (mJ/m <sup>2</sup> )	$\gamma_s^+$ (mJ/m <sup>2</sup> )	$\gamma_s^-$ (mJ/m <sup>2</sup> )
<b>iGC columns<sup>a</sup></b> (iGC-C)					
<b>PTFE</b>	19.5 ± 2.3	19.1 ± 2.3	0.4 ± 0.0	0.1 ± 0.0	0.5 ± 0.1
<b>PE</b>	32.2 ± 2.1	31.6 ± 2.1	0.6 ± 0.0	0.1 ± 0.0	0.9 ± 0.2
<b>PA</b>	43.8 ± 1.8	41.9 ± 1.7	1.9 ± 0.2	0.2 ± 0.1	4.1 ± 2.5
<b>Glass</b>	46.7 ± 1.6	39.8 ± 1.8	7.0 ± 0.3	0.5 ± 0.2	22.8 ± 1.8
<b>iGC film-cell<sup>b</sup></b> (iGC-FC)					
<b>PTFE</b>	21.1 ± 3.1	21.0 ± 3.2	0.1 ± 0.1	0.0 ± 0.0	0.5 ± 0.3
<b>PE</b>	32.9 ± 1.5	31.0 ± 1.5	1.9 ± 0.6	0.3 ± 0.3	2.7 ± 1.2
<b>PA</b>	48.5 ± 2.3	44.7 ± 2.6	3.8 ± 1.2	0.4 ± 0.3	8.9 ± 1.7
<b>Glass</b>	47.9 ± 3.3	40.0 ± 2.2	7.8 ± 1.1	2.5 ± 2.1	11.0 ± 2.6
<b>Contact angle<sup>b</sup></b> (CA)					
<b>PTFE</b>	17.1 ± 0.9	15.9 ± 0.6	1.2 ± 0.3	0.2 ± 0.1	1.9 ± 0.5
<b>PE</b>	32.5 ± 2.7	29.3 ± 1.5	3.2 ± 1.2	0.8 ± 0.3	3.4 ± 1.6
<b>PA</b>	42.4 ± 0.9	40.4 ± 0.8	2.0 ± 0.2	0.1 ± 0.0	11.5 ± 1.5
<b>Glass</b>	56.2 ± 0.3	39.4 ± 1.6	16.8 ± 1.9	1.3 ± 0.3	54.1 ± 0.2

376